Research Square

Preprints are preliminary reports that have not undergone peer review. They should not be considered conclusive, used to inform clinical practice, or referenced by the media as validated information.

Comparative genomics reveals the adaptive evolutionary basis of golden-yellow coloration in the large yellow croaker

Shuo Jia
Zhejiang Ocean University
Peng Zheng
Zhejiang Ocean University
Lihua Jiang
florencejiang@126.com

Zhejiang Ocean University
Xiaolong Ying
Zhoushan Fisheries Research Institute
Jialang Zheng
Zhejiang Ocean University
Yifan Liu
Zhejiang Ocean University
Weihua Song
Zhejiang Ocean University
Kun Jia
Zhejiang Ocean University
Yuxiang Zhu
Pingyang Institute of Science and Technology Innovation
Jiantong Feng
Zhejiang Ocean University
Xiaojun Yan
Zhejiang Ocean University

Research Article

Keywords: Large yellow croaker, comparative genomics, body coloration, positive selection, gene-family expansion, carotenoids

Posted Date: October 15th, 2026

DOI: https://doi.org/10.21203/rs.3.rs-11050589/v1

License: This work is licensed under a Creative Commons Attribution 4.0 International License.
Read Full License

Additional Declarations: No competing interests reported.

Comparative genomics reveals the adaptive evolutionary basis of golden-yellow coloration in the large yellow croaker

Shuo Jia[1] , Peng Zheng[1] , Lihua Jiang[1,2]*, Xiaolong Yin[3] , Jialang Zheng[1] , Yifan Liu[1] , Weihua Song[1] , Kun Jia[1] , Yuxiang Zhu[2], Jiantong Feng[1], Xiaojun Yan[1] *

1. National Engineering Research Center of Marine Facilities Aquaculture, Zhejiang Ocean University, No. 1 Haida South Road, Dinghai District, Zhoushan, 316022, China

2. Pingyang Institute of Science and Technology Innovation, No. 8 Binjiang Avenue, Aojiang Town, Pingyang, Wenzhou, 325400, China

3. Zhoushan Fisheries Research Institute, Zhoushan, China, No. 28 Tiyu Road, Dinghai District, Zhoushan, 316021, China

*Correspondence: florencejiang@126.com (Lihua Jiang); yanxj@zjou.edu.cn (Xiaojun Yan)

Abstract

The golden-yellow pigmentation on the body surface of adult large yellow croaker (*Larimichthys crocea*) is hypothesized to play roles in conspecific recognition, environmental adaptation, and visual signaling in natural ecosystems, while also constituting a key trait affecting its commercial value. In this study, we integrated genomic resources from eight species, including Sciaenids, and conducted homologous gene family clustering, phylogenetic reconstruction, divergence time estimation, and chromosome-level synteny analysis to assess genomic structural conservation. Furthermore, gene family expansion/contraction analyses, positive selection detection using branch-site models, and functional enrichment (GO/KEGG) were systematically employed to screen candidate genes and pathways associated with body coloration, alongside amino acid site comparisons and protein structural localization analysis of the candidate gene *npc1l1*. Our results revealed that while the sciaenid genomes are generally conserved at the macro-structural level, the *L. crocea* lineage exhibits specific evolutionary signals related to golden pigmentation. A total of 11,470 shared gene families were identified across the eight species, with only four unique families in *L. crocea*. Phylogenetic and syntenic analyses confirmed the closest relationship with L. polyactis and demonstrated overall genomic stability among closely related Sciaenids.

In the *L. crocea* lineage, 88 gene families showed significant expansion and 22 showed contraction; expanded genes were enriched in pigmentation regulation and lipid metabolism, yielding candidates such as *cers2*, *cers3*, *hspa8*, and *bax*. Positive selection analysis detected 688 genes under selection, significantly enriched in intestinal cholesterol absorption, lipid digestion, and organic hydroxy compound transport, from which candidates including *npc1l1*, *npc1*, *bscl2*, *elovl5*, *mc1r*, *edn1*, *cd63*, *bloc1s5*, and *ltk* were identified. Notably, among the two positively selected sites in *npc1l1*, the 77th amino acid resides within the Niemann-Pick C1 N-terminus domain, suggesting a potential role in the adaptive evolution of carotenoid absorption. Collectively, these findings imply that the golden coloration in *L. crocea* may result from a combination of optimized carotenoid uptake, transport, and storage, alongside melanin regulation and optical enhancement mediated by iridophores. This study provides comparative genomic insights into the evolutionary characteristics of coloration-related genes in *L. crocea*, enriches the molecular understanding of fish pigmentation mechanisms, and lays a foundation for future research and selective breeding targeting body color traits in this species.

Keywords: Large yellow croaker; comparative genomics; body coloration; positive selection; gene-family expansion; carotenoids

Introduction

The large yellow croaker (*Larimichthys crocea*) is an important economic fish species in China's coastal waters, occurring mainly in the East China Sea, Yellow Sea, and adjacent waters and playing important roles in marine fisheries and stock enhancement and aquaculture (Song et al., 2024). Adults generally display a conspicuous golden-yellow body surface. This phenotype is not only a major external characteristic but is also closely associated with ecological processes such as intraspecific recognition, environmental adaptation, and visual signaling. At the same time, body-surface yellow coloration is not completely constant; it varies in response to light, circadian rhythms, and other environmental factors, suggesting joint regulation by intrinsic genetic mechanisms and external conditions (Han et al., 2018; Lin et al.,

2026). For aquaculture and consumer markets, coloration is also an important trait affecting product appearance and economic value (Zheng et al., 2025b; Vissio et al., 2021). Therefore, elucidating the molecular basis of golden-yellow coloration from genetic and evolutionary perspectives is important for understanding phenotypic regulation and improving related traits.

Sciaenidae is species-rich and exhibits diversity in coloration, ecological habits, and adaptive traits, providing a valuable system for comparative studies of coloration-related traits. Compared with other Sciaenids, the adult large yellow croaker generally displays a more pronounced golden-yellow coloration, with high distinctiveness and representativeness, suggesting that its coloration formation and maintenance may rely on molecular features that differ from those of closely related species. Because closely related species share recent phylogenetic relationships and relatively similar genomic backgrounds, placing the large yellow croaker within a comparative framework of Sciaenidae can help identify lineage-specific genetic signals associated with its golden-yellow coloration.

Fish coloration and its maintenance generally involve differentiation and distribution of multiple chromatophore types, pigment synthesis and transport, and coordinated action of related regulatory genes. The formation of yellow or golden-yellow coloration often depends not only on the uptake, transport, and deposition of pigments such as carotenoids but also on the masking effect of the melanin system and optical properties mediated by iridophores (Luo et al., 2021; Funt et al., 2017; Sköld et al., 2016). In the large yellow croaker, existing studies have focused mainly on nutritional regulation of coloration, particularly the effects of dietary carotenoid sources and composition on skin yellowness and pigment deposition. For example, changes in the dietary lutein/canthaxanthin ratio have been shown to significantly affect skin yellowness, redness, and carotenoid content. Skin yellowness and carotenoid levels are positively correlated with the dietary proportion of lutein, whereas higher canthaxanthin levels are more conducive to increasing skin redness (Yi et al., 2015).

Another study comparing skin pigment composition between wild and cultured large yellow croaker found that wild fish had more pronounced yellow skin and higher carotenoid accumulation; it further indicated that carotenoid storage in the skin is closely associated with lutein esterification (Zheng et al., 2025a; Mellado-Ortega and Hornero-Mendez, 2017). More recently, morphological, pigment-biochemical, and proteomic analyses of diurnal body-color variation in the large yellow croaker provided additional evidence that coloration is influenced not only by nutrient supply but also by dynamic regulatory processes (Lin et al., 2026). Nevertheless, existing research remains largely focused on nutritional, physiological, and phenotypic regulation, and a systematic understanding of the genetic basis of golden-yellow coloration—particularly the lineage-specific molecular evolutionary mechanisms revealed in comparisons among closely related Sciaenids is still lacking. Thus, studies limited to nutritional regulation or localized functional analyses in a single species are insufficient to fully elucidate the molecular basis of golden-yellow coloration from an evolutionary perspective.

Comparative genomics provides a framework for systematically identifying conserved and lineage-specific molecular signals associated with trait divergence among closely related species. Homologous gene-family clustering, phylogenetic analysis, divergence-time estimation, and synteny analysis can be used to evaluate conservation of genome structure and evolutionary relationships; when combined with gene-family expansion and contraction analyses, positive-selection tests, and functional enrichment analyses, these approaches facilitate the identification of candidate genes and potential regulatory pathways associated with specific phenotypes. Accordingly, placing the large yellow croaker within a comparative framework that includes Sciaenids and outgroup species may help elucidate the molecular basis of its golden-yellow coloration from an evolutionary perspective (Lu and Luo, 2020; Houston et al., 2020; Ellegren, 2014; Demuth and Hahn, 2009; Yanez et al., 2015). Here, we integrated genome resources from multiple sciaenid and outgroup species and performed

comparative genomic analyses, including phylogenetic, synteny, gene-family evolutionary, and positive-selection analyses, to identify candidate genes and pathways associated with golden-yellow coloration in the large yellow croaker and to provide a theoretical basis for subsequent functional validation and mechanistic studies.

Materials and methods

Genomic data acquisition

We selected eight species as study taxa: European seabass (*Dicentrarchus labrax*) (NCBI, 2021), large yellow croaker (*Larimichthys crocea*) (NCBI, 2018), *Pennahia pawak* (NCBI, 2024a), *Collichthys lucidus* (NCBI, 2019), barramundi (*Lates calcarifer*) (NCBI, 2022), small yellow croaker (*Larimichthys polyactis*) (NCBI, 2024b), *Nibea albiflora* (NCBI, 2020), and red drum (*Sciaenops ocellatus*) (NCBI, 2023). Sciaenid species were used for comparisons among closely related taxa, whereas European seabass and barramundi served as outgroups to assist phylogenetic inference and evolutionary analyses. Reference genome assemblies, protein sequences, and gene-annotation files for all species were obtained from public databases. To ensure comparability across species, sequence names, gene identifiers, and annotation formats were standardized.

Homologous gene family identification

Homologous gene families were identified from protein sequences of the eight species using OrthoFinder (Emms and Kelly, 2019) to infer orthologous and paralogous relationships. Sequence-similarity searches were performed with DIAMOND using an E-value threshold of 1×10^{-5}. High-confidence homologous relationships were retained and used to define gene-family clusters. The resulting gene-family assignments were then used to quantify shared and species-specific gene families and the distribution of family copy numbers across species.

Phylogenetic analysis and divergence-time estimation

Single-copy orthologs were selected from the identified homologous gene families for phylogenetic analysis. Protein sequences were first aligned with MAFFT, and codon-level alignments were generated from the corresponding coding sequences.

144 Gblocks was then used to retain conserved alignment blocks, thereby reducing the
145 influence of low-quality regions on phylogenetic inference. A species tree was
146 constructed by maximum likelihood using RAxML, and bootstrap support was used to
147 assess the reliability of the topology. Finally, divergence times and evolutionary
148 relationships among species were estimated with the mcmctree program in the PAML
149 package using time-calibration information (Katoh and Standley, 2013; Castresana,
150 2000; Stamatakis, 2014; Yang, 2007).

151 **Genome synteny analysis**

152 To evaluate conservation of genome structure among closely related Sciaenids, we
153 performed synteny analysis using chromosome-level genomes and annotation files
154 from *P. pawak*, the small yellow croaker, and the large yellow croaker. Coding
155 sequences were first extracted from the genome sequences and annotation files, and
156 chromosome identifiers and gene-annotation formats were standardized to ensure
157 comparability. The JCVI toolkit was then used to identify syntenic blocks from
158 homologous-gene matches, and dot plots and chromosome-level visualizations were
159 used to assess chromosome correspondences and local structural rearrangements (Tang
160 et al., 2024).

161 **Gene family expansion and contraction analysis**

162 Gene-family expansion and contraction were analyzed using gene-family copy
163 numbers, the species tree, and divergence-time estimates. We first counted gene copies
164 in each homologous family for each species and constructed a gene-family copy-
165 number matrix. CAFE was then used with a stochastic birth-death model to analyze
166 changes in family size and identify expansions or contractions on individual
167 evolutionary branches. A conditional p-value was calculated for each family, and $p <$
168 0.05 was used to define significant expansion or contraction. These analyses yielded
169 branch-specific expansion and contraction events and their significance, from which
170 significantly changed families were selected. GO and KEGG enrichment analyses were
171 subsequently performed for significantly expanded and contracted families using the R
172 package clusterProfiler (functions enrichGO and enrichKEGG). Multiple testing was

173 corrected with the Benjamini – Hochberg method, and an adjusted p-value of $P < 0.05$
174 was used as the significance threshold for identifying enriched GO terms and KEGG
175 pathways and for interpreting the potential biological significance of gene-family
176 changes (Mendes et al., 2020; Yu et al., 2012).

177 **Positive selection analysis**

178 To identify positively selected genes on different evolutionary branches, we
179 analyzed codon alignments of single-copy orthologs with the codeml program in the
180 PAML package. Based on the phylogeny, the branch containing the large yellow
181 croaker, small yellow croaker, and *C.lucidus* was designated the foreground branch,
182 and the remaining sciaenid species were designated background branches. Positive
183 selection on the specified branch was tested using the branch-site model. We fitted an
184 alternative model (Model A) that permits positive selection and a null model that does
185 not, and compared their goodness of fit with a likelihood-ratio test (LRT). A *p*-value
186 was calculated for each gene, and genes with $p < 0.05$ were initially considered
187 candidate positively selected genes. Multiple testing was then corrected using the
188 Benjamini-Hochberg method to control the false discovery rate; genes with an adjusted
189 $P < 0.05$ were retained as the final set of robust positively selected genes. Key sites
190 under positive selection were identified using the Bayes empirical Bayes (BEB) method
191 to investigate potential molecular mechanisms underlying protein functional evolution.
192 GO and KEGG enrichment analyses were performed for positively selected genes in
193 the three foreground species with clusterProfiler, using $P < 0.05$ as the significance
194 threshold (Yang, 2007; Yu et al., 2012). At the protein-sequence level, ESPript 3.2 was
195 used to visualize multiple-sequence alignments and assess conservation of candidate-
196 gene amino-acid sequences. At the structural level, the SWISS-MODEL server was
197 used to predict three-dimensional structures of candidate proteins, and PyMOL v3.1.4.1
198 was used for visualization and generation of three-dimensional models to aid
199 interpretation of the structural and functional significance of key sites.

200

201 **Results**

Gene family clustering analysis

Homologous gene-family clustering of protein sequences from the eight species identified 11,470 gene families shared by all species, indicating a high degree of conservation in gene composition among Sciaenids and the outgroups (Fig. 1). The numbers of species-specific gene families varied among species: only four were identified in the large yellow croaker, compared with 110 in the small yellow croaker and 212 in *C.lucidus*, indicating relatively limited divergence in the species-specific gene complement of the large yellow croaker. Statistical analysis of gene-family composition (Table 1) showed that the large yellow croaker genome contains 22,816 genes, of which 22,812 (99.98%) were successfully assigned to 17,759 gene families; only four genes were not assigned to any family. The four large-yellow-croaker-specific gene families contained eight genes in total. Compared with other Sciaenids, the large yellow croaker has relatively few unclustered genes and species-specific gene families, further indicating high similarity between its gene composition and that of closely related species.Overall, Sciaenids showed strong conservation at the gene-family level, and the small number of large-yellow-croaker-specific gene families suggests that important phenotypic differences, such as surface pigment deposition, are more likely to result from functional differentiation or regulatory changes within conserved gene families than from the emergence of large numbers of novel gene families.

The phylogenetic relationships of the eight species were systematically inferred from a species tree constructed using single-copy orthologs (Fig. 2). Sciaenids formed a clear set of phylogenetic branches; the large yellow croaker and small yellow croaker were the closest relatives, diverging approximately 16.19 Ma and together forming a sister group with *C.lucidus*. This clade originated approximately 20.25 Ma. In another lineage, *N.albiflora* and *P.pawak* diverged approximately 27.86 Ma and subsequently formed a higher-level clade with *S. ocellatus* at approximately 46.99 Ma. The entire sciaenid group diverged from a common ancestor shared with the outgroups, barramundi and European seabass, approximately 113.60 Ma, indicating a clear hierarchical evolutionary relationship among the study taxa.Taken together, the phylogenetic

topology and divergence-time estimates indicate that the close relationship and relatively recent divergence between the large and small yellow croakers may underlie their high genomic similarity, whereas differences in coloration-related traits are more likely to reflect adaptive evolution after divergence. The clade comprising the large yellow croaker, small yellow croaker, and *C. lucidus* also provides the phylogenetic basis for defining the foreground branch in subsequent positive-selection analyses.

Genome synteny analysis results

To further evaluate conservation of genome structure among closely related Sciaenids, we performed chromosome-level synteny analysis of the large yellow croaker, *P.pawak*, and the small yellow croaker (Fig. 3). All three species have 24 chromosomes and show extensive chromosome-level synteny, with clear one-to-one correspondences for most chromosomes. At the whole-genome level, synteny was closest between the large and small yellow croakers, with gene order highly conserved across most chromosome regions. By contrast, *P.pawak* showed some structural differences from the other two species in several chromosome regions. Nevertheless, the three species retained a high degree of overall structural consistency, with only localized rearrangements, such as possible inversions or translocations, observed.

Overall, closely related Sciaenids exhibit strong structural conservation at the chromosome level, and the large and small yellow croakers show the highest degree of syntenic concordance, consistent with the phylogenetic results. These findings indicate that the large yellow croaker has not undergone large-scale restructuring of the genome during evolution. Its phenotypic differences, including surface pigment deposition, are therefore more likely to arise from evolution of key genes and their regulatory networks than from chromosome-scale structural changes.

Gene family expansion and contraction and functional enrichment analysis

Using gene-family copy numbers and phylogenetic relationships, we analyzed gene-family expansions and contractions on the branches of the eight species with CAFE (Fig. 4). During the evolution of the large yellow croaker, 88 gene families were significantly expanded and 22 were significantly contracted ($p < 0.05$), indicating substantial changes in gene-family size in specific functional directions.

Functional annotation and enrichment analysis of significantly expanded gene families (Figs. 5 and 6) showed that these genes were primarily enriched in biological processes closely related to coloration, including positive regulation of developmental pigmentation, regulation of developmental pigmentation, and regulation of pigmentation. Expanded families were also significantly enriched in lipid-related processes, including lipid storage, positive regulation of lipid biosynthesis, and negative regulation of lipid catabolism. At the molecular-function and pathway levels, these genes were also associated with cytochrome P450 and sphingolipid signaling pathways, which are closely related to lipid metabolism and cellular signal regulation.

Gene annotation identified several candidate genes associated with lipid metabolism and cellular homeostasis among the significantly expanded families, including *cers2*, *cers3*, *hspa8*, and *bax*. These genes participate in sphingolipid synthesis, lipid metabolic regulation, and apoptosis, respectively, and may indirectly contribute to the deposition and regulation of coloration-related substances by influencing lipid synthesis, transport, and intracellular homeostasis.Overall, expanded gene families in the large yellow croaker lineage were concentrated mainly in pigmentation regulation and lipid-metabolism functions, suggesting that its golden-yellow phenotype is related not only to pigment production but also to regulation of lipid synthesis, storage, and metabolism.

Positive-selection genes and their protein-sequence and structural features

Positive-selection analysis based on the branch-site model was performed for the branches containing the large yellow croaker, small yellow croaker, and *C.lucidus*. A total of 688 positively selected genes (PSGs) were detected on the large yellow croaker

foreground branch. Functional enrichment analysis (Figs. 7 and 8) showed that these genes were primarily enriched in intestinal cholesterol absorption, lipid digestion, and organic hydroxy compound transport, indicating that lipid-related metabolism and transport experienced substantial selection pressure in this lineage.Functional annotation of the positively selected genes identified several classes of candidates associated with coloration. *mc1r* and *edn1* were under positive selection in melanogenesis and melanin regulation and may participate in regulation of melanin synthesis. *cd63* and *bloc1s5* were under positive selection in melanosome formation and transport, suggesting adaptive changes in pigment-granule formation and trafficking. In addition, LTK is associated with iridophore differentiation, and its positive-selection signal suggests that regulation of optical structures may contribute to body coloration.

Several key genes involved in lipid metabolism and carotenoid-related processes showed significant positive-selection signals, including *npc1l1* and *npc1*, which participate in intestinal cholesterol absorption; *bscl2*, which participates in lipid-droplet formation; and *elovl5*, *agpat3*, *cerk*, *apoa1bp*, and *abca12*, which participate in lipid metabolism and transport. Functionally, these genes cover multiple stages, including uptake of lipophilic substances, intracellular transport, and tissue distribution.Analysis of amino-acid sites in positively selected genes (Table 2) identified multiple sites with high posterior probabilities. In *npc1l1*, significant positive-selection signals were detected at amino-acid positions 77 and 932. Multiple-sequence alignment showed that the large yellow croaker, small yellow croaker, and *C. lucidus* all carry proline (P) at position 77, whereas other Sciaenids carry glutamate (E); at position 932, the three focal species carry arginine (R), whereas the other species carry valine (V) (Fig. 9).Protein-structure prediction showed that amino acid 77 is located within the Niemann–Pick C1 N-terminal domain of NPC1L1, a functional region important for cholesterol recognition and binding (Fig. 10). This substitution may affect the local three-dimensional conformation and thereby alter the interaction properties of the protein

with lipophilic substrates. Overall, the positively selected genes were functionally involved in lipid metabolism, pigment production, and cellular structural regulation and showed adaptive changes at both the sequence and structural levels, suggesting that they may jointly regulate coloration-related traits in the large yellow croaker.

Discussion

The results of homologous gene-family clustering, phylogenetic analysis and divergence-time estimation, and synteny analysis indicate that Sciaenids are generally highly conserved at the genomic level. A total of 11,470 gene families were shared by the eight species, whereas only four were specific to the large yellow croaker. This pattern suggests that its coloration is more likely to reflect functional differentiation and adaptive evolution within a conserved genetic background than to be driven by the emergence of numerous novel gene families. Phylogenetic analysis placed the large yellow croaker and small yellow croaker as sister taxa that diverged approximately 16.19 million years ago, suggesting that part of their coloration-related molecular basis may have arisen during the divergence of these closely related lineages. Synteny analysis further showed that the large yellow croaker, *P.pawak*, and small yellow croaker each have 24 chromosomes and retain strong chromosome-level correspondence, with only limited local rearrangements. Thus, the coloration-related traits of the large yellow croaker are more likely associated with sequence variation in key genes, gene-family expansion and contraction, and adaptive selection than with large-scale genome restructuring. Against this broadly conserved genomic background, the expanded gene families and positively selected genes identified below are more likely to represent molecular evolutionary signals associated with coloration.

Our results indicate that golden-yellow coloration in adult large yellow croaker is not determined by a single factor but by the coordinated action of multiple molecular mechanisms, principally carotenoid absorption, transport, and storage; regulation of melanin deposition; and iridophore-mediated optical modulation. Carotenoid deposition provides the material basis for yellow coloration, melanin affects its

345 apparent intensity through masking, and iridophores further enhance surface brightness
346 and visual contrast by modulating light reflection and scattering. These mechanisms are
347 functionally coupled and together produce the stable and conspicuous golden-yellow
348 phenotype of adult large yellow croaker.

349 At the adult stage, the golden-yellow coloration of the large yellow croaker is
350 derived mainly from carotenoid deposition in xanthophores. Lutein has been shown to
351 be the predominant carotenoid component in the skin and is closely associated with the
352 degree of surface yellowness (Yi et al., 2014; Lin et al., 2026). Fish generally cannot
353 synthesize carotenoids de novo, so their carotenoids are acquired primarily through the
354 diet (Sathyaruban et al., 2021). As a typical lipophilic molecule, lutein depends heavily
355 on lipid-metabolism systems for absorption, transport, and tissue distribution and often
356 occurs in esterified forms, which improve stability in hydrophobic environments and
357 promote tissue accumulation (Mellado-Ortega and Hornero-Mendez, 2017). Thus,
358 efficient carotenoid deposition in vivo depends not only on the amount ingested but
359 also on coordinated molecular processes involved in lipid transport and storage.

360 During carotenoid deposition, intestinal lutein absorption is a critical determinant
361 of the efficiency of its accumulation in vivo. As a lipophilic molecule, lutein uptake
362 across intestinal epithelial cells depends on lipid-transport proteins; NPC1L1 is
363 considered a central mediator of lutein absorption. Previous work shows that NPC1L1
364 mediates not only cholesterol absorption but also transmembrane transport of
365 xanthophylls such as lutein, and that changes in its activity can substantially affect
366 intestinal lutein-absorption efficiency (During et al., 2005). In the present study, *npc1l1*
367 showed significant positive-selection signals. Multiple-sequence alignment showed
368 that the large yellow croaker, small yellow croaker, and *C.lucidus* carry proline (P) at
369 position 77, whereas the other Sciaenids carry glutamate (E); at position 932, the three
370 focal species carry arginine (R), whereas the other species carry valine (V). Position 77
371 lies within the Niemann–Pick C1 N-terminal domain, an important region for
372 recognition and binding of cholesterol and other lipophilic substrates by NPC1L1. The

373 glutamate-to-proline substitution may alter the local conformation and thereby affect
374 substrate binding and transmembrane transport efficiency. Given the role of NPC1L1
375 in lutein absorption, these lineage-specific substitutions may improve lutein recognition
376 and transport, thereby increasing carotenoid uptake. NPC1, an important intracellular
377 cholesterol-transport factor, participates in lipid trafficking through the endosome–
378 lysosome pathway (Gong et al., 2016) and may assist redistribution after lutein enters
379 the cell.

380 After intestinal absorption, redistribution and tissue deposition of lutein depend on
381 an effective lipid-transport and storage system. At the levels of intracellular trafficking
382 and tissue distribution, lipid-transport-related genes including *npc1*, *apoa1bp*, and
383 *abca12* were under positive selection, suggesting adaptive optimization of lutein
384 transport within cells and across tissues. NPC1 participates in endosome–lysosome
385 lipid trafficking, APOA1BP affects cholesterol efflux by modulating the lipoprotein
386 microenvironment, and ABCA12 plays important roles in lipid efflux and cutaneous
387 lipid transport. Together, these processes may facilitate efficient lutein transport and
388 redistribution among tissues (Fang and Miller, 2019; Akiyama, 2014).

389 At the storage level, lipid droplets are the principal intracellular storage structures
390 for lipophilic molecules and are critical for stable carotenoid accumulation. In this study,
391 the core lipid-droplet-biogenesis gene *bscl2* and several lipid-metabolism genes,
392 including *agpat3*, *elovl5*, and *cerk*, were under positive selection, suggesting adaptive
393 optimization of lipid-droplet formation and lipid-metabolic regulation in the large
394 yellow croaker. By participating in lipid synthesis, fatty-acid elongation, and
395 sphingolipid metabolism, these genes may jointly establish a stable lipid
396 microenvironment that provides a structural basis for long-term accumulation of lutein
397 and other lipophilic molecules (Salo et al., 2016; Wilfling et al., 2013; Jakobsson et al.,
398 2006; Sugiura et al., 2002).

399 Moreover, *cers2* and *cers3*, identified among the expanded gene families, also
400 participate in sphingolipid metabolism and may further stabilize carotenoids in tissues

401 by modulating the cell membrane and local cutaneous lipid environment. Overall, the
402 positively selected and expanded genes span multiple key steps from carotenoid uptake
403 to deposition, forming a continuous molecular chain of "absorption–transport–storage"
404 that may systematically improve lutein deposition in vivo (Silva et al., 2012;
405 Jennemann et al., 2012).

406 Beyond carotenoid deposition efficiency, the final visual appearance of yellow
407 coloration in adult large yellow croaker is strongly regulated by the melanin system.
408 Melanin and xanthophyll pigments are both chemical pigments whose coloration
409 depends on light absorption and reflection, but melanin has a particularly strong light-
410 absorbing capacity. When melanin deposition decreases, its masking effect on yellow
411 pigments in underlying or adjacent regions is reduced, making carotenoid-derived
412 yellow coloration more conspicuous. Changes in melanin deposition therefore have an
413 important role in regulating surface-color contrast.

414 At the level of melanogenesis and its regulation, key genes including *mc1r*, *edn1*,
415 and *dkk1* were under positive selection. MC1R is a core receptor in the melanogenic
416 pathway that regulates intracellular signal transduction in melanocytes and affects
417 melanin synthesis. EDN1 is an important paracrine factor that can influence melanocyte
418 proliferation and pigment production, whereas DKK1, an antagonist of Wnt signaling,
419 can suppress melanocyte activity and reduce pigment production when upregulated.
420 Positive selection on these genes may influence the intensity of surface melanin
421 deposition through coordinated regulation of the melanogenic pathway (Gross et al.,
422 2009; Yamaguchi and Hearing, 2009; Sun et al., 2018).

423 At the level of melanosome formation and transport, *bloc1s5* and *cd63* were also
424 under positive selection. BLOC1S5 is an important component of the BLOC-1 complex
425 and participates in the biogenesis and cargo sorting of lysosome-related organelles,
426 including melanosomes; CD63 participates in melanosome structural formation and
427 protein sorting. Functional changes in these genes may affect melanosome maturation
428 and pigment-transport efficiency, thereby further regulating melanin distribution and

429 deposition in the skin (Goff et al., 2025; Van Niel et al., 2011).

430 Among the expanded gene families, *hspa8* and *bax* may also participate in the
431 regulation of the melanin system. HSPA8 is a molecular chaperone that has important
432 roles in protein folding and autophagy, and autophagy is closely linked to melanosome
433 degradation and maintenance of pigment-granule homeostasis. BAX is a pro-apoptotic
434 regulator whose expression may affect the balance between melanocyte survival and
435 renewal. Expansion of these genes may therefore indirectly alter surface melanin
436 content by regulating melanocyte fate and pigment-granule homeostasis. Overall,
437 coordinated action of melanogenesis regulators, melanosome-biogenesis genes, and
438 cellular homeostasis factors may reduce the masking effect of melanin and enhance the
439 visual expression of carotenoid-derived yellow coloration, making the surface golden-
440 yellow phenotype more prominent (Bonam et al., 2019; Park et al., 2025; Kim et al.,
441 2000).

442 In addition to chemical pigments, iridophores strongly affect surface-color
443 brightness and optical properties. Their regularly arranged intracellular reflective
444 structures reflect and scatter incident light, thereby increasing surface brightness and
445 color contrast. In the present study, *ltk*, a key regulator of iridophore differentiation and
446 development, was under positive selection. Loss of LTK function has been reported to
447 cause abnormal iridophore development or even iridophore absence, substantially
448 altering surface reflectance. Adaptive changes in LTK may therefore enhance
449 iridophore formation or function and increase reflection of incident light, making
450 carotenoid-derived yellow coloration brighter and more conspicuous (Lopes et al.,
451 2008).

452 From an evolutionary perspective, the positive selection and expansion detected
453 in genes related to lipid metabolism, pigment synthesis, and cellular structural
454 regulation may be closely associated with the adaptive evolution of the large yellow
455 croaker in its ecological environment. Light conditions, depth variation, and differences
456 in background environment in the marine habitat may impose persistent selection on

body coloration, thereby driving coordinated evolution of genes involved in carotenoid-deposition efficiency and pigment-contrast regulation. Such coordinated adaptation across multiple genes and pathways may constitute an important evolutionary basis for the stable golden-yellow surface phenotype of the large yellow croaker.

Previous studies indicate that yellow or yellow-orange coloration in other fishes is mainly associated with carotenoid uptake, accumulation, and storage in xanthophores; *scarb1* and *plin6* are representative key genes. In zebrafish, thyroid hormone promotes xanthophore maturation and carotenoid-dependent coloration, while SCARB1 is closely associated with carotenoid accumulation in xanthophores (Saunders et al., 2019). PLIN6 has been shown to localize to the surface of carotenoid droplets in xanthophores, where it participates in the enrichment and transport of lipophilic pigments (Granneman et al., 2017). Studies in Nile tilapia further show that PLIN6 loss markedly reduces carotenoid content and coloration intensity in xanthophores, whereas XDH loss has relatively little effect on overall coloration. This finding suggests that, in some teleosts, carotenoid metabolism and storage may be more important for yellow coloration than pteridine synthesis (Liang et al., 2025).

Our results provide new molecular evidence for the mechanism underlying yellow coloration in the large yellow croaker. Previous studies have linked NPC1L1 closely to intestinal lutein absorption and identified *bscl2* as a key gene in lipid storage and lipid-droplet formation (During et al., 2005; Salo et al., 2016). Both genes were under positive selection in the large yellow croaker, indicating that their related functions may have been enhanced during adaptive evolution. Specifically, positive selection on *npc1l1* may increase the uptake of lutein and other pigment molecules, thereby increasing the pigment supply required for yellow coloration; positive selection on *bscl2* may promote lipid-droplet formation and maintenance, creating a more favorable cellular environment for carotenoid accumulation and stable storage. Thus, adaptive evolution of *npc1l1* and *bscl2* may act at two key stages-pigment absorption and storage-and jointly enhance the golden-yellow coloration trait. Whereas previous

485 studies have emphasized SCARB1-mediated pigment uptake and PLIN6-associated
486 lipid-droplet stabilization, our findings add NPC1L1 and BSCL2 as complementary
487 components acting at the initial stage of intestinal lutein absorption and at lipid-droplet
488 formation, respectively. This further supports the view that golden-yellow coloration of
489 the large yellow croaker involves coordinated optimization of the continuous
490 carotenoid "absorption–transport–storage" process.

491 Taken together, our results indicate that the golden-yellow coloration of adult large
492 yellow croaker is produced by the coordinated action of multiple molecular
493 mechanisms. At the material level, deposition of carotenoids, particularly lutein,
494 provides the principal source of yellow pigment, and its absorption, transport, and
495 storage are systematically optimized through lipid-metabolism and lipid-droplet-
496 formation systems. At the regulatory level, adaptive changes in genes involved in
497 melanogenesis and melanosome transport may reduce the masking effect of melanin
498 and thereby increase the visibility of yellow pigment. Changes in iridophore-related
499 genes may further enhance surface brightness and visual contrast by increasing light
500 reflection and scattering. These mechanisms act synergistically to form a multilayer
501 regulatory system comprising "pigment deposition–masking regulation–optical
502 enhancement" (Fig.11), producing the stable and conspicuous golden-yellow
503 phenotype of adult large yellow croaker.

504

505 **Conclusion**

506 Using genomic data from multiple Sciaenids and outgroup species, we
507 systematically performed homologous gene-family clustering, phylogenetic, synteny,
508 gene-family expansion and contraction, and positive-selection analyses to
509 comprehensively characterize the molecular evolutionary mechanisms underlying
510 coloration-related traits from a comparative-genomics perspective.

511 The results show that Sciaenids are generally highly conserved at the genomic
512 level, with many shared gene families and few large-yellow-croaker-specific families.
513 This indicates that differences in coloration are not attributable to the emergence of

514 novel gene families but are more likely to reflect functional differentiation and adaptive
515 evolution within a conserved genomic background. Synteny analysis also showed
516 strong chromosome-level concordance among the large yellow croaker, small yellow
517 croaker, and *P.pawak*, further supporting the stability of genome structure during
518 evolution.

519 At the functional level, significant gene-family expansions and positive-selection
520 signals were detected in the large yellow croaker lineage. These genes were primarily
521 enriched in pigmentation regulation, lipid metabolism, and related signaling pathways.
522 Key candidate genes, including *npc1l1*, *npc1*, *bscl2*, *mc1r*, *edn1*, and *ltk*, participate in
523 carotenoid absorption, lipid transport and storage, melanin regulation, and iridophore
524 development. The amino-acid substitution detected in a functional domain of NPC1L1
525 suggests that this protein may have undergone adaptive optimization for uptake of
526 lipophilic pigments.

527 Together, these analyses indicate that the golden-yellow coloration of the large
528 yellow croaker is not driven by a single factor but results from the coordinated action
529 of carotenoid deposition, melanin regulation, and iridophore-mediated optical effects.
530 These processes form a multilayer coloration-regulatory system centered on carotenoid
531 absorption, transport, and storage; supported by regulation of melanin deposition; and
532 enhanced by iridophore-mediated optical effects.

533

534 **CRediT authorship contribution statement**

535 Lihua Jiang and Shuo Jia: Conceptualization, Methodology, Investigation, Formal
536 analysis, Data curation; Writing-original draft and Writing-review; Peng Zheng:
537 Investigation, Data curation; Xiaolong Yin and Jialang Zheng: Investigation, Image
538 processing, funding and project administration; Yifan Liu and Weihua Song:
539 Investigation, Validation; Kun Jia: Resources, Sample collection; Yuxiang Zhu:
540 Funding acquisition, Resources; Jiantong Feng: Formal analysis; Lihua Jiang and
541 Xiaojun Yan: Supervision, Funding acquisition, Writing-review and editing.

542

Declaration of competing interest

The authors declare that they have no known competing financial interests or personal relationships that could have appeared to influence the work reported in this paper.

Funding Declaration

This work is supported by the Aquaculture Breeding and Seedling Technology Innovation Center Project of Zhoushan (2025Y001-1), Zhejiang Provincial Science and Technology Plan Project- "Pioneer and Leading Goose+X" Research and Development Program (2026C02A3020), National Key Research and Development Program of China Grants (2023YFD2401900), National Key R&D Program of China (2023YFD2401905).

References

Akiyama, M., 2014. The roles of ABCA12 in epidermal lipid barrier formation and keratinocyte differentiation. Biochimica et Biophysica Acta 1841(3), 435–440.

Bonam, S.R., Ruff, M., Muller, S., 2019. HSPA8/HSC70 in immune disorders: a molecular rheostat that adjusts chaperone-mediated autophagy substrates. Cells 8(8), 849.

Castresana, J., 2000. Selection of conserved blocks from multiple alignments for their use in phylogenetic analysis. Molecular Biology and Evolution 17(4), 540–552.

Demuth, J.P., Hahn, M.W., 2009. The life and death of gene families. BioEssays 31, 29–39.

During, A., Dawson, H.D., Harrison, E.H., 2005. Carotenoid transport is decreased and expression of the lipid transporters SR-BI, NPC1L1, and ABCA1 is downregulated in Caco-2 cells treated with ezetimibe. Journal of Nutrition 135(10), 2305–2312.

Ellegren, H., 2014. Genome sequencing and population genomics in non-model organisms. Trends in Ecology & Evolution 29(1), 51–63.

Emms, D.M., Kelly, S., 2019. OrthoFinder: phylogenetic orthology inference for comparative genomics. Genome Biology 20, 238.

Fang, L., Miller, Y.I., 2019. Regulation of lipid rafts, angiogenesis and inflammation by AIBP. Current Opinion in Lipidology 30(3), 218–223.

Funt, N., Palmer, B.A., Weiner, S., et al., 2017. Koi fish-scale iridophore cells orient guanine crystals to maximize light reflection. ChemPlusChem 82(6), 914–923.

Goff, P.S., Patel, S., Harper, D.C., et al., 2025. Reprogramming of endolysosomes for melanogenesis in BLOC-1-deficient melanocytes. Current Biology 35(15), 3570–3586.

Gong, X., Qian, H., Zhou, X., et al., 2016. Structural insights into the Niemann-Pick C1 (NPC1)-mediated cholesterol transfer and Ebola infection. Cell 165(6), 1467–1478.

Granneman, J.G., Kimler, V.A., Zhang, H., et al., 2017. Lipid droplet biology and evolution illuminated by the characterization of a novel perilipin in teleost fish. eLife 6, e21771.

Gross, J.B., Borowsky, R., Tabin, C.J., 2009. A novel role for Mc1r in the parallel evolution of depigmentation in independent populations of the cavefish Astyanax mexicanus. PLOS Genetics 5(1), e1000326.

Han, Z., Lv, C., Xiao, S., et al., 2018. Transcriptome Profiling of the Abdominal Skin of *Larimichthys crocea* in Light Stress. J Ocean Univ China 17, 344–354.

Houston, R.D., Bean, T.P., Macqueen, D.J., et al., 2020. Harnessing genomics to fast-track genetic improvement in aquaculture. Nature Reviews Genetics 21, 389–409.

Jakobsson, A., Westerberg, R., Jacobsson, A., 2006. Fatty acid elongases in mammals: their regulation and roles in metabolism. Progress in Lipid Research 45(3), 237–249.

Jennemann, R., Rabionet, M., Gorgas, K., et al., 2012. Loss of ceramide synthase 3 causes lethal skin barrier disruption. Human Molecular Genetics 21(3), 586–608.

Katoh, K., Standley, D.M., 2013. MAFFT multiple sequence alignment software version 7: improvements in performance and usability. Molecular Biology and Evolution 30(4), 772–780.

Kim, Y.G., Kim, H.J., Kim, D.S., et al., 2000. Up-regulation and redistribution of Bax in ultraviolet B-irradiated melanocytes. Pigment Cell Research 13(5), 352–357.

Liang, G., Yao, J., Wu, J., et al., 2025. Carotenoids, instead of pteridines, determine color of xanthophores and erythrophores in tilapia. Journal of Heredity 116(4), 466–478.

605 Lin, N., Wu, J., Deng, H., et al., 2026. Body coloration characterization and proteomic analysis of
606 diurnal color variation in farmed *Larimichthys crocea*. Animals 16(3), 353.
607 Lopes, S.S., Yang, X., Müller, J., et al., 2008. Leukocyte tyrosine kinase functions in pigment cell
608 development. PLOS Genetics 4(3), e1000026.
609 Lu, G.Q., Luo, M.K., 2020. Genomes of major fishes in world fisheries and aquaculture: Status,
610 application and perspective. Aquaculture and Fisheries 5(4), 163–173.
611 Luo, M., Lu, G., Yin, H., et al., 2021. Fish pigmentation and coloration: Molecular mechanisms and
612 aquaculture perspectives. Reviews in Aquaculture 13, 2395–2440.
613 Mellado-Ortega, E., Hornero-Mendez, D., 2017. Lutein esterification in wheat flour increases the
614 carotenoid retention and is induced by storage temperatures. Foods 6(12).
615 Mendes, F.K., Vanderpool, D., Fulton, B., et al., 2020. CAFE 5 models variation in evolutionary
616 rates among gene families. Bioinformatics 36(22–23), 5516–5518.
617 NCBI, 2018. GenBank assembly GCF_000972845.2.
618 https://www.ncbi.nlm.nih.gov/datasets/genome/GCF_000972845.2/ (accessed 6 March 2026).
619 NCBI, 2019. GenBank assembly GCA_004119915.2.
620 https://www.ncbi.nlm.nih.gov/datasets/genome/GCA_004119915.2/ (accessed 6 March 2026).
621 NCBI, 2020. GenBank assembly GCA_014281875.1.
622 https://www.ncbi.nlm.nih.gov/datasets/genome/GCA_014281875.1/ (accessed 6 March 2026).
623 NCBI, 2021. GenBank assembly GCF_905237075.1.
624 https://www.ncbi.nlm.nih.gov/datasets/genome/GCF_905237075.1/ (accessed 10 March 2026).
625 NCBI, 2022. GenBank assembly GCF_001640805.2.
626 https://www.ncbi.nlm.nih.gov/datasets/genome/GCF_001640805.2/ (accessed 10 March 2026).
627 NCBI, 2023. GenBank assembly GCA_033000465.1.
628 https://www.ncbi.nlm.nih.gov/datasets/genome/GCA_033000465.1/ (accessed 10 March 2026).
629 NCBI, 2024a. GenBank assembly GCA_042310395.1.
630 https://www.ncbi.nlm.nih.gov/datasets/genome/GCA_042310395.1/ (accessed 10 March 2026).
631 NCBI, 2024b. GenBank assembly GCA_040670005.1.
632 https://www.ncbi.nlm.nih.gov/datasets/genome/GCA_040670005.1/ (accessed 10 March 2026).
633 Park, N.Y., Kim, S.H., Jo, D.S., et al., 2025. Emerging perspectives on the selective autophagy of
634 melanosomes: melanophagy. Experimental & Molecular Medicine 57, 2709–2716.
635 Salo, V.T., Belevich, I., Li, S., et al., 2016. Seipin regulates ER-lipid droplet contacts and cargo
636 delivery. EMBO Journal 35(24), 2699–2716.
637 Sathyaruban, S., Uluwaduge, D.I., Yohi, S., et al., 2021. Potential natural carotenoid sources for the
638 colouration of ornamental fish: a review. Aquaculture International 29, 1507–1528.
639 Saunders, L.M., Mishra, A.K., Aman, A.J., et al., 2019. Thyroid hormone regulates distinct paths to
640 maturation in pigment cell lineages. eLife 8, e45181.
641 Silva, L.C., Ben David, O., Pewzner-Jung, Y., et al., 2012. Ablation of ceramide synthase 2 strongly
642 affects biophysical properties of membranes. Journal of Lipid Research 53(3), 430–436.
643 Sköld, H.N., Aspengren, S., Cheney, K.L., et al., 2016. Fish chromatophores —from molecular
644 motors to animal behavior. International Review of Cell and Molecular Biology 321, 171–219.
645 Song, W., Li, L.Z., Xie, W.M., et al., 2024. Investigation of the current status and development
646 pathways of the large yellow croaker aquaculture industry. China Fisheries 11, 5. [in Chinese].

Stamatakis, A., 2014. RAxML version 8: a tool for phylogenetic analysis and post-analysis of large phylogenies. Bioinformatics 30(9), 1312–1313.

Sugiura, M., Kono, K., Liu, H., et al., 2002. Ceramide kinase, a novel lipid kinase. Molecular cloning and functional characterization. Journal of Biological Chemistry 277(26), 23294–23300.

Sun, Q., Rabbani, P., Takeo, M., et al., 2018. Dissecting Wnt signaling for melanocyte regulation during wound healing. Journal of Investigative Dermatology 138(7), 1591–1600.

Tang, H., Krishnakumar, V., Zeng, X., et al., 2024. JCVI: a versatile toolkit for comparative genomics analysis. iMeta 3(4), e211.

Van Niel, G., Charrin, S., Simoes, S., et al., 2011. The tetraspanin CD63 regulates ESCRT-independent and-dependent endosomal sorting during melanogenesis. Developmental Cell 21(4), 708–721.

Vissio, P.G., Darias, M.J., Di Yorio, M.P., et al., 2021. Fish skin pigmentation in aquaculture: the influence of rearing conditions and its neuroendocrine regulation. General and Comparative Endocrinology 301, 113662.

Wilfling, F., Wang, H., Haas, J.T., et al., 2013. Triacylglycerol synthesis enzymes mediate lipid droplet growth by relocalizing from the ER to lipid droplets. Developmental Cell 24(4), 384–399.

Yamaguchi, Y., Hearing, V.J., 2009. Physiological factors that regulate skin pigmentation. Biofactors 35(2), 193–199.

Yanez, J.M., Newman, S., Houston, R.D., 2015. Genomics in aquaculture to better understand species biology and accelerate genetic progress. Frontiers in Genetics 6, 128.

Yang, Z., 2007. PAML 4: phylogenetic analysis by maximum likelihood. Molecular Biology and Evolution 24(8), 1586–1591.

Yi, X.W., Li, J., Xu, W., et al., 2015. Effects of dietary xanthophylls/astaxanthin ratios on the growth and skin pigmentation of large yellow croaker *Larimichthys crocea* (Richardson, 1846). J Appl Ichthyol 31, 780–786.

Yi, X.W., Xu, W., Zhou, H.H., et al., 2014. Effects of dietary astaxanthin and xanthophylls on the growth and skin pigmentation of large yellow croaker *Larimichthys croceus.* Aquaculture 433, 377–383.

Yu, G., Wang, L.G., Han, Y., et al., 2012. clusterProfiler: an R package for comparing biological themes among gene clusters. OMICS 16(5), 284–287.

Zheng, J.L., Yan, X.J., Wu, Y.Y., et al., 2025b. Quality grading of large yellow croaker. Journal of Fisheries of China 49(8), 089618. [in Chinese].

Zheng, J.L., Zhu, T., Jin, W.Y., et al., 2025a. Comparative analysis of carotenoids, fatty acids, minerals, tastes, and odor in the skin of wild versus farmed large yellow croaker: Superior nutritional benefits with elevated heavy metal risks. Aquaculture 594, 741471.

Table 1. Summary of gene family clustering and species-specific gene statistics for sciaenid fishes and outgroup species

Species	No of genes	Genes in orthologous clusters	Gene families	Species-specific gene families	Species-specific genes
Collichthys lucidus	25582	25514	16788	212	459
Dicentrarchus labrax	23325	23310	17814	32	104
Lates calcarifer	24324	24306	17771	62	197
Larimichthys crocea	22816	22812	17759	4	8
Larimichthys polyactis	22341	22340	17421	110	559
Nibea albiflora	18788	18760	15266	80	207
Pennahia pawak	25092	23505	17999	56	257
Sciaenops ocellatus	22589	22560	17250	17	75

Table 2. Positively selected genes detected in Sciaenidae based on the branch-site model

Gene	Branch *p*-Value	Locus, Information	Gene Family
BLOC1S5	1.19E-03	137, K, 0.958*	OG11625
MC1R	1.99E-02	16, I, 0.963*	OG06949
LTK	4.80E-03	112, Y, 0.983*	OG05284
CD63	2.45E-02	138, K, 0.953*	OG08632
DKK1	4.65E-11	55, F, 0.972* 62, S, 0.950*	OG11095
BSCL2	3.26E-03	401, N, 0.988*	OG07745
NPC1	2.01E-12	645, K, 0.992**	OG04701
NPC1L1	4.29E-06	77, P, 0.966* 1024, R, 0.963*	OG04642
ELOVL5	3.45E-03	244, T, 0.956* 254, L, 0.983*	OG11058
AGPAT3	3.50E-02	287, N, 0.954*	OG06320
CERK	1.46E-10	63, S, 0.975* 64, Q, 0.994**	OG14971
APOA1BP	2.36E-02	151, N, 0.971*	OG14837
ABCA12	1.27E-06	3895, K, 0.952*	OG02627
EDN1	2.62E-13	158, Y, 0.978*	OG14774

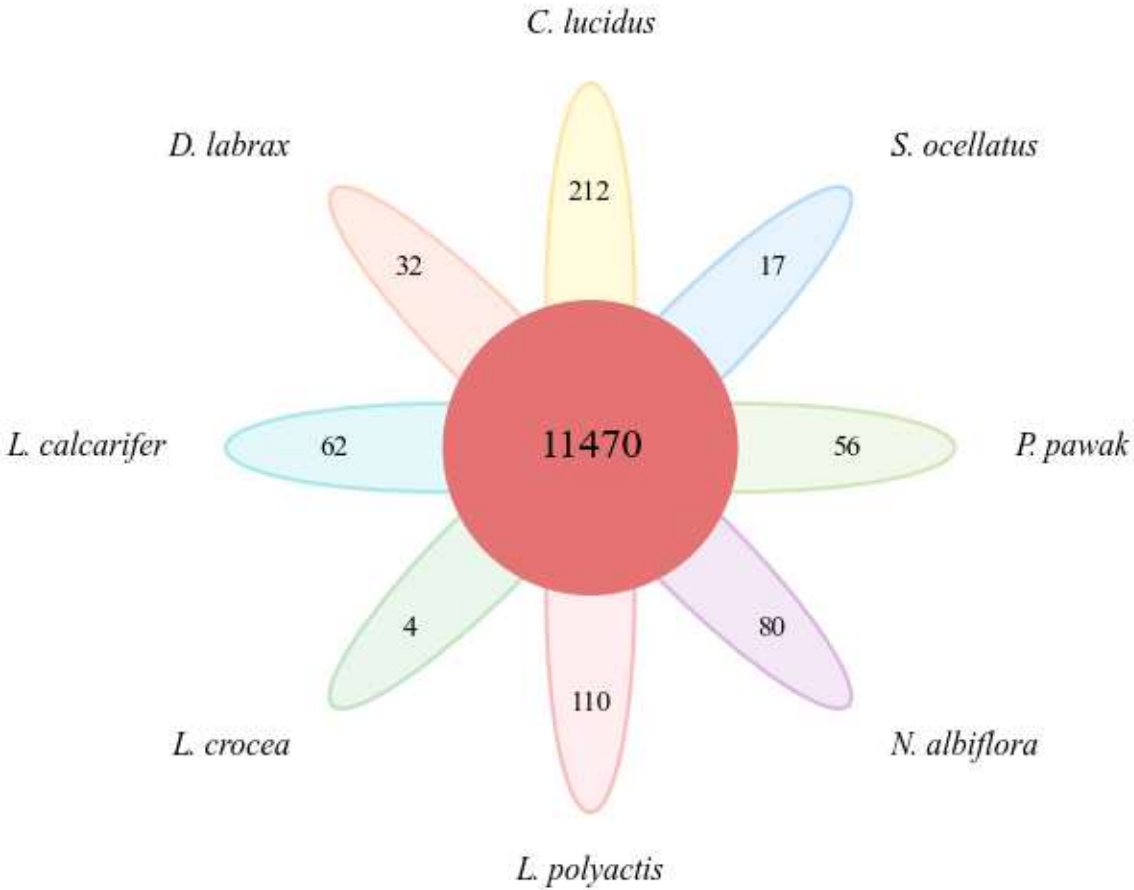
C. lucidus
212
S. ocellatus
17
P. pawak
56
N. albiflora
80
L. polyactis
110
L. crocea
4
L. calcarifer
62
D. labrax
32
11470

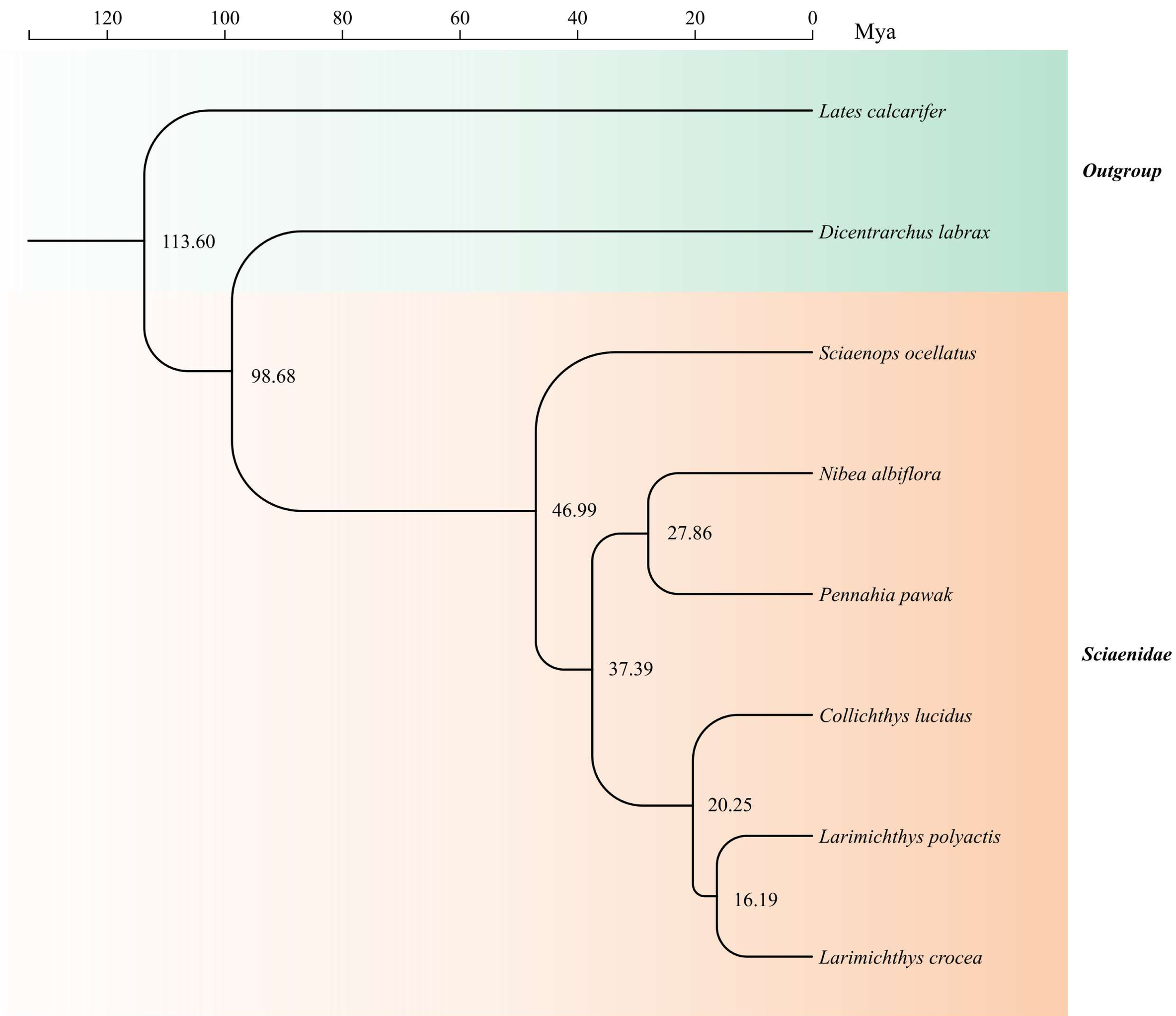

Tree scale 10

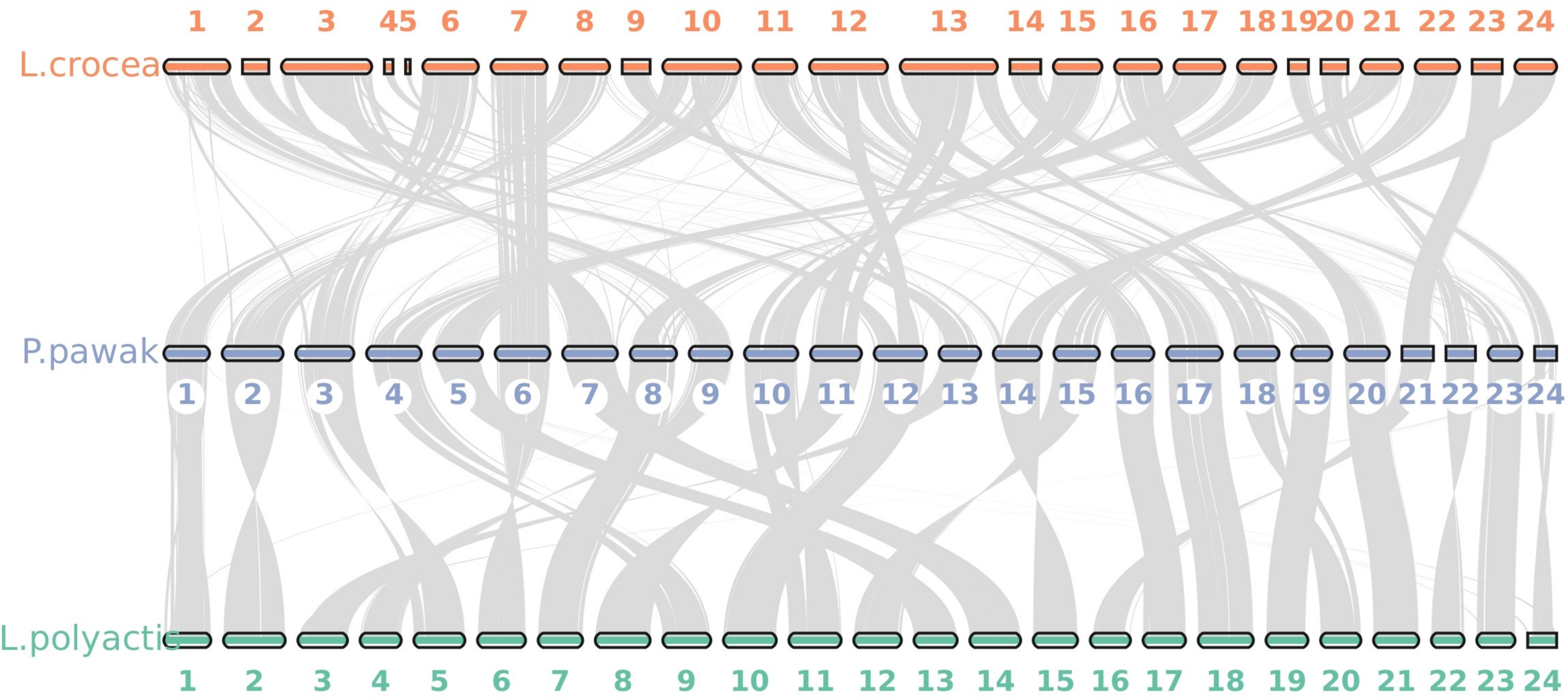
L.crocea
1 2 3 45 6 7 8 9 10 11 12 13 14 15 16 17 18 19 20 21 22 23 24
P.pawak
1 2 3 4 5 6 7 8 9 10 11 12 13 14 15 16 17 18 19 20 21 22 23 24
L.polyactis
1 2 3 4 5 6 7 8 9 10 11 12 13 14 15 16 17 18 19 20 21 22 23 24

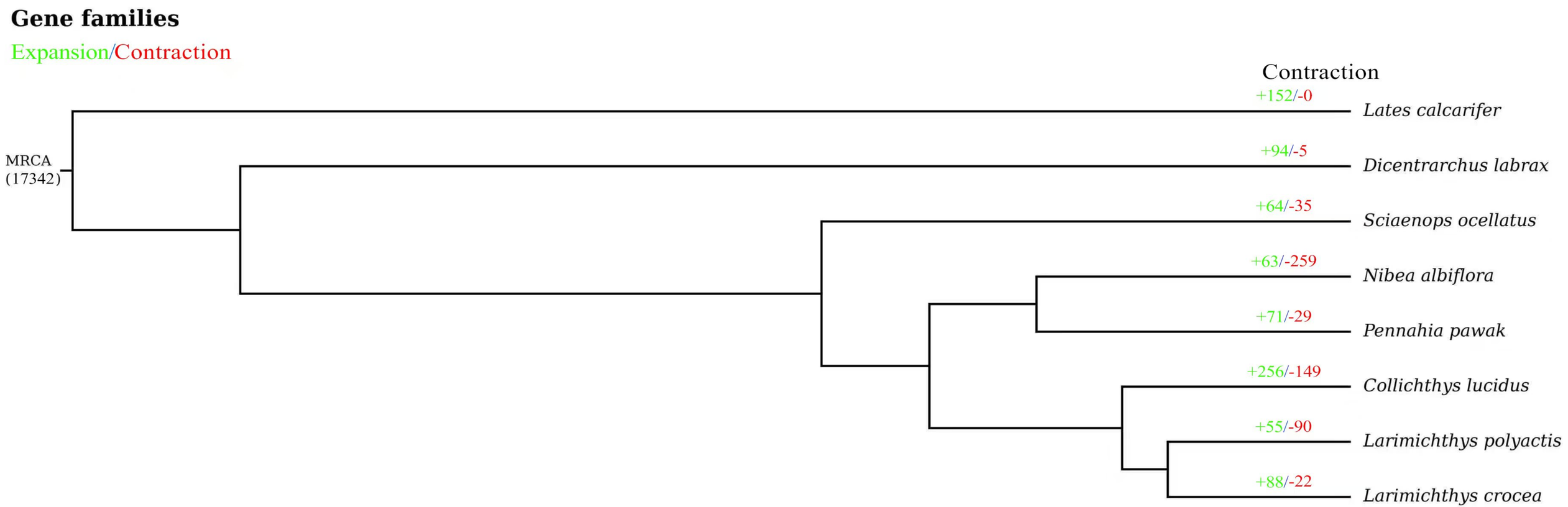
Gene families
Expansion/Contraction
Contraction
MRCA
(17342)
+152/-0
Lates calcarifer
+94/-5
Dicentrarchus labrax
+64/-35
Sciaenops ocellatus
+63/-259
Nibea albiflora
+71/-29
Pennahia pawak
+256/-149
Collichthys lucidus
+55/-90
Larimichthys polyactis
+88/-22
Larimichthys crocea

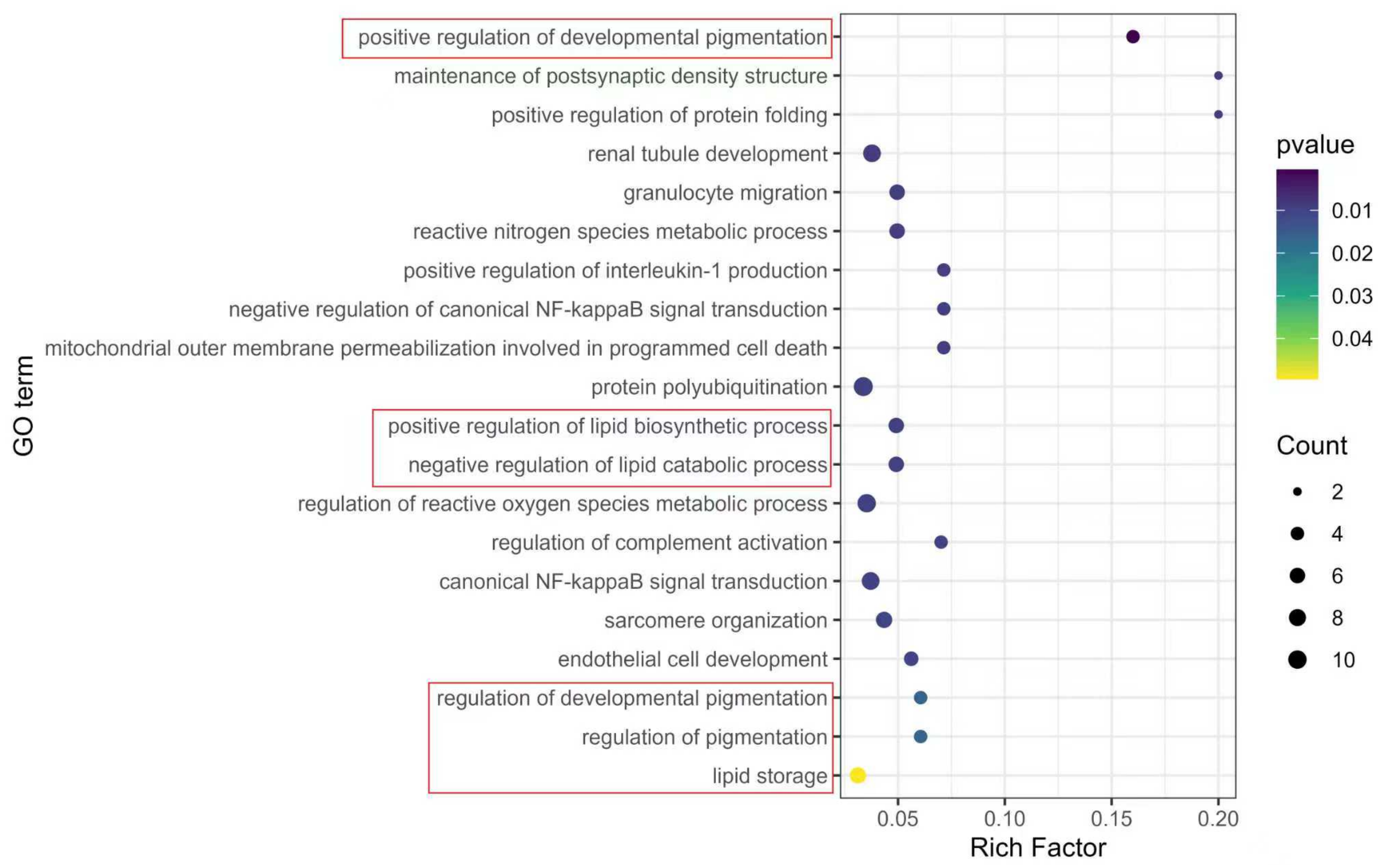
positive regulation of developmental pigmentation
maintenance of postsynaptic density structure
positive regulation of protein folding
renal tubule development
granulocyte migration
reactive nitrogen species metabolic process
positive regulation of interleukin-1 production
negative regulation of canonical NF-kappaB signal transduction
mitochondrial outer membrane permeabilization involved in programmed cell death
protein polyubiquitination
positive regulation of lipid biosynthetic process
negative regulation of lipid catabolic process
regulation of reactive oxygen species metabolic process
regulation of complement activation
canonical NF-kappaB signal transduction
sarcomere organization
endothelial cell development
regulation of developmental pigmentation
regulation of pigmentation
lipid storage
GO term
0.05
0.10
0.15
0.20
Rich Factor
pvalue
0.01
0.02
0.03
0.04
Count
2
4
6
8
10

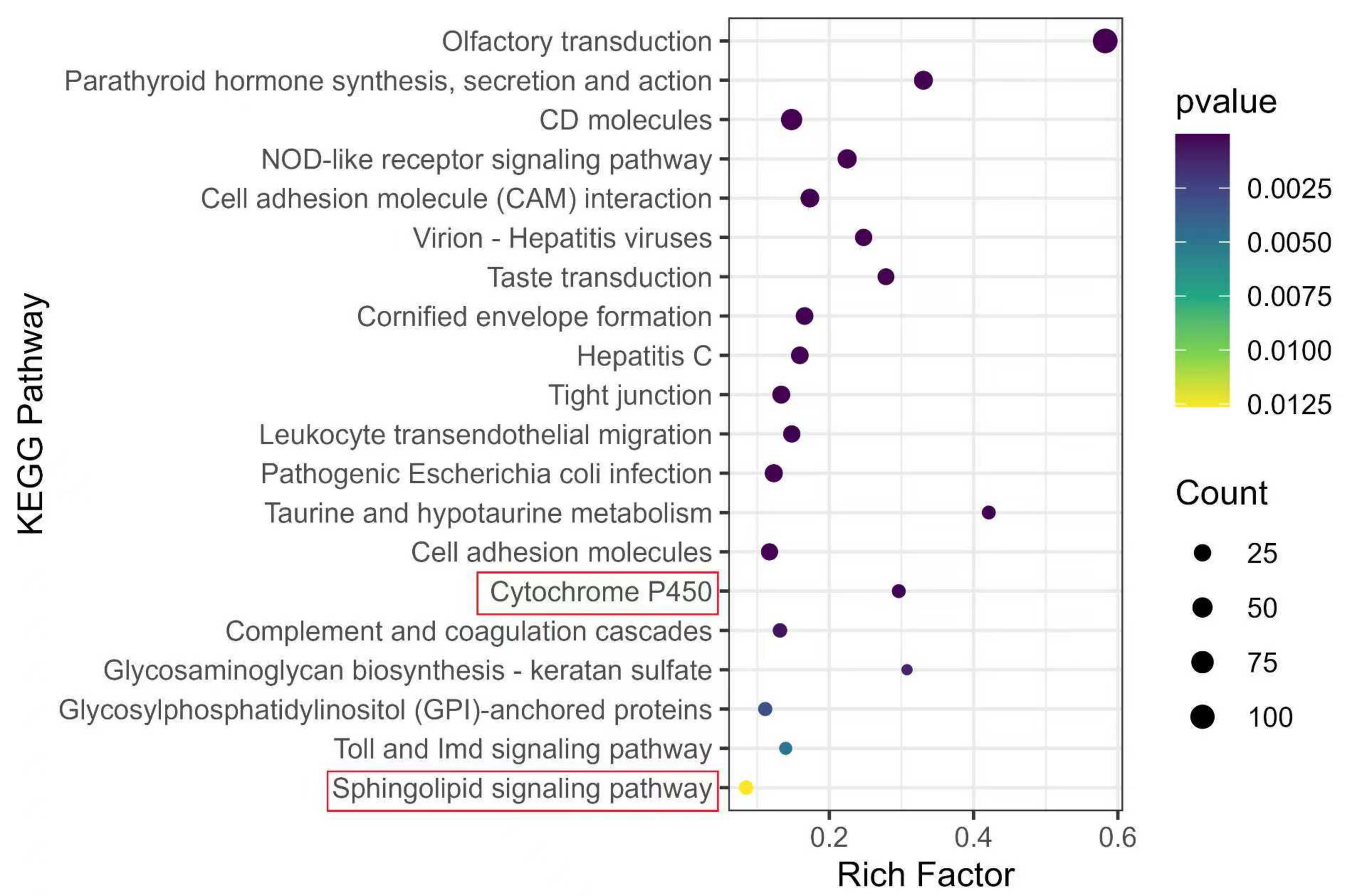
Olfactory transduction
Parathyroid hormone synthesis, secretion and action
CD molecules
NOD-like receptor signaling pathway
Cell adhesion molecule (CAM) interaction
Virion - Hepatitis viruses
Taste transduction
Cornified envelope formation
Hepatitis C
Tight junction
Leukocyte transendothelial migration
Pathogenic Escherichia coli infection
Taurine and hypotaurine metabolism
Cell adhesion molecules
Cytochrome P450
Complement and coagulation cascades
Glycosaminoglycan biosynthesis - keratan sulfate
Glycosylphosphatidylinositol (GPI)-anchored proteins
Toll and Imd signaling pathway
Sphingolipid signaling pathway
KEGG Pathway
0.2
0.4
0.6
Rich Factor
pvalue
0.0025
0.0050
0.0075
0.0100
0.0125
Count
25
50
75
100

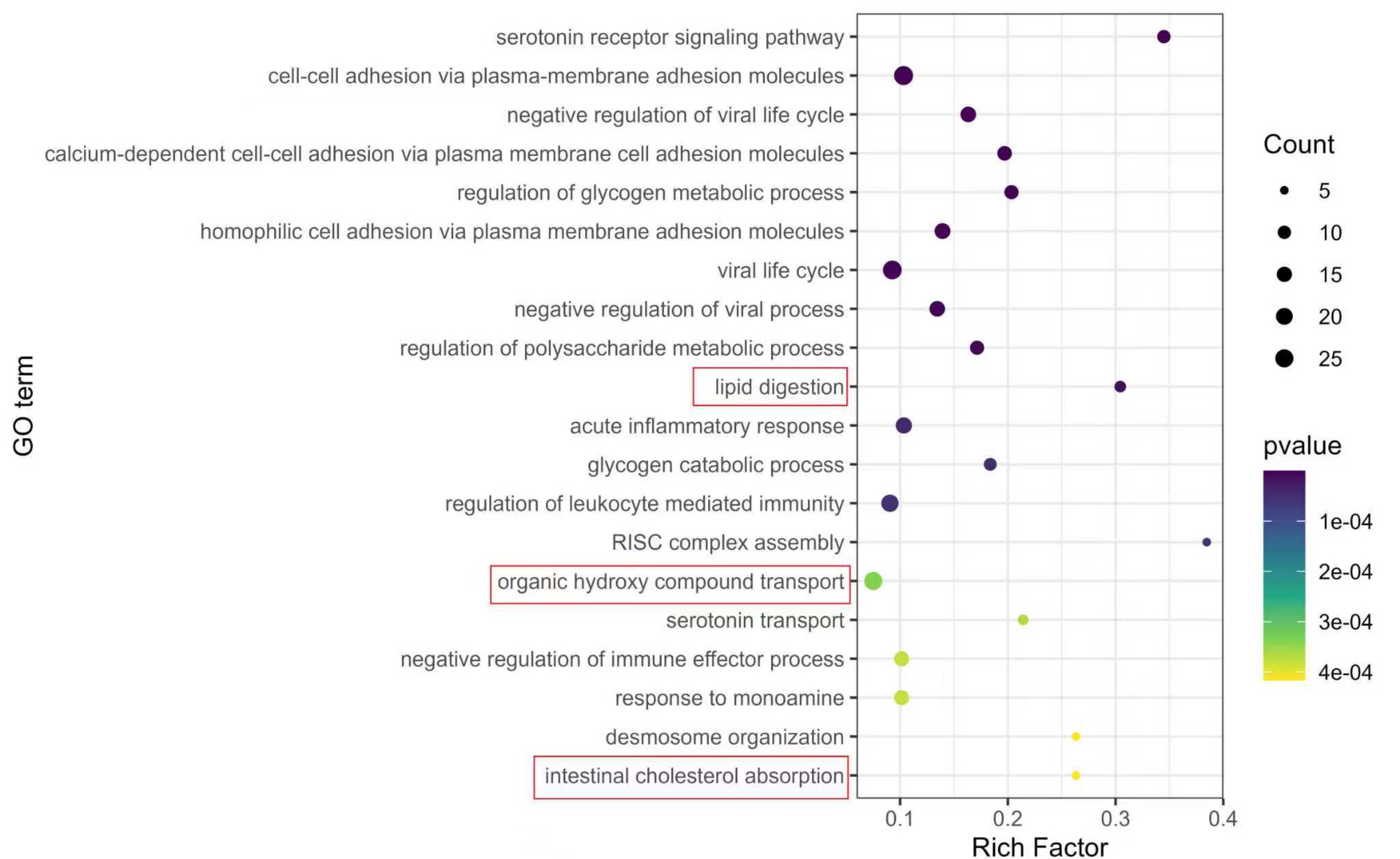
serotonin receptor signaling pathway
cell-cell adhesion via plasma-membrane adhesion molecules
negative regulation of viral life cycle
calcium-dependent cell-cell adhesion via plasma membrane cell adhesion molecules
regulation of glycogen metabolic process
homophilic cell adhesion via plasma membrane adhesion molecules
viral life cycle
negative regulation of viral process
regulation of polysaccharide metabolic process
lipid digestion
acute inflammatory response
glycogen catabolic process
regulation of leukocyte mediated immunity
RISC complex assembly
organic hydroxy compound transport
serotonin transport
negative regulation of immune effector process
response to monoamine
desmosome organization
intestinal cholesterol absorption
GO term
0.1
0.2
0.3
0.4
Rich Factor
Count
5
10
15
20
25
pvalue
1e-04
2e-04
3e-04
4e-04

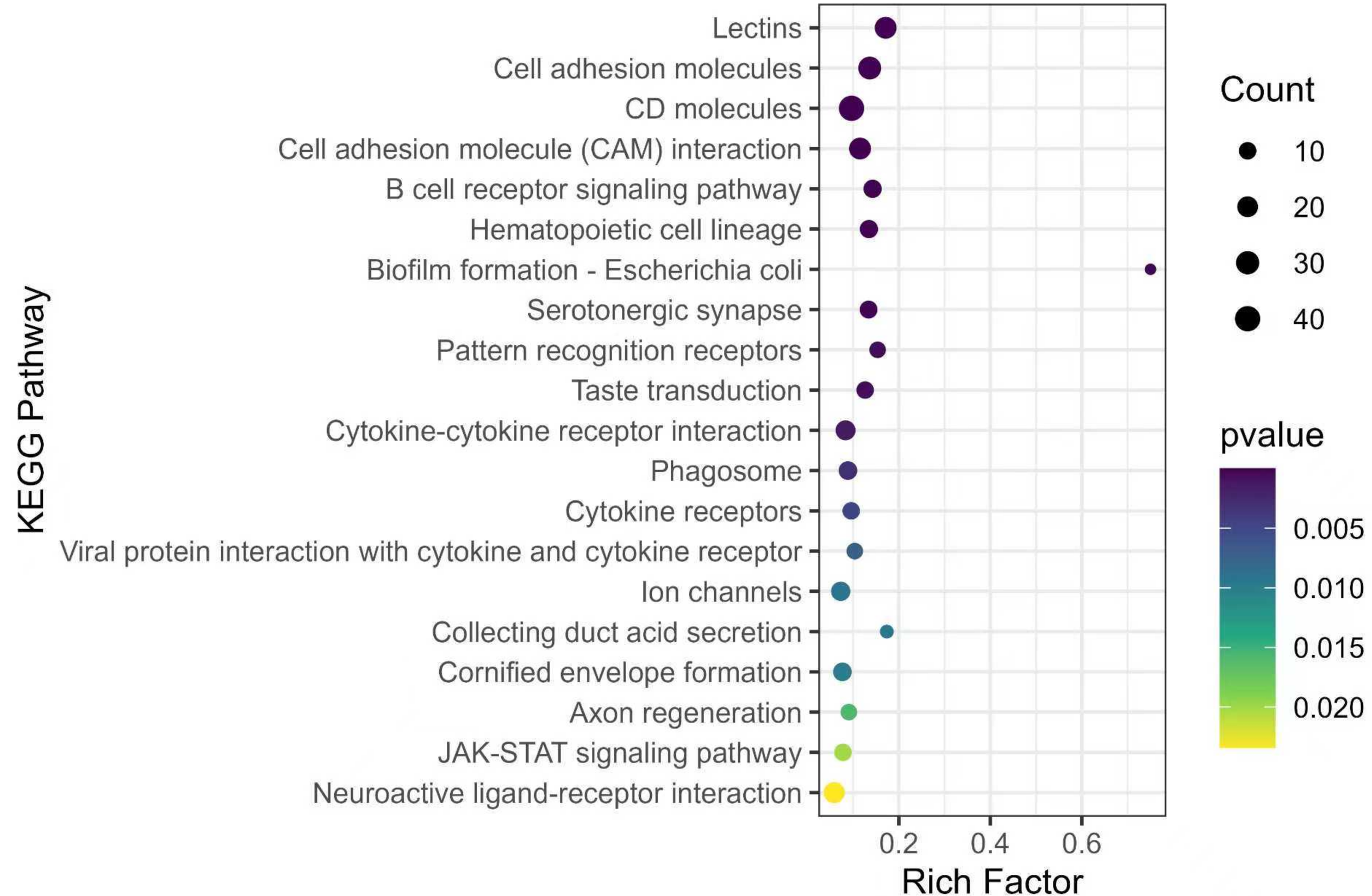
KEGG Pathway
Lectins
Cell adhesion molecules
CD molecules
Cell adhesion molecule (CAM) interaction
B cell receptor signaling pathway
Hematopoietic cell lineage
Biofilm formation - Escherichia coli
Serotonergic synapse
Pattern recognition receptors
Taste transduction
Cytokine-cytokine receptor interaction
Phagosome
Cytokine receptors
Viral protein interaction with cytokine and cytokine receptor
Ion channels
Collecting duct acid secretion
Cornified envelope formation
Axon regeneration
JAK-STAT signaling pathway
Neuroactive ligand-receptor interaction
0.2
0.4
0.6
Rich Factor
Count
10
20
30
40
pvalue
0.005
0.010
0.015
0.020

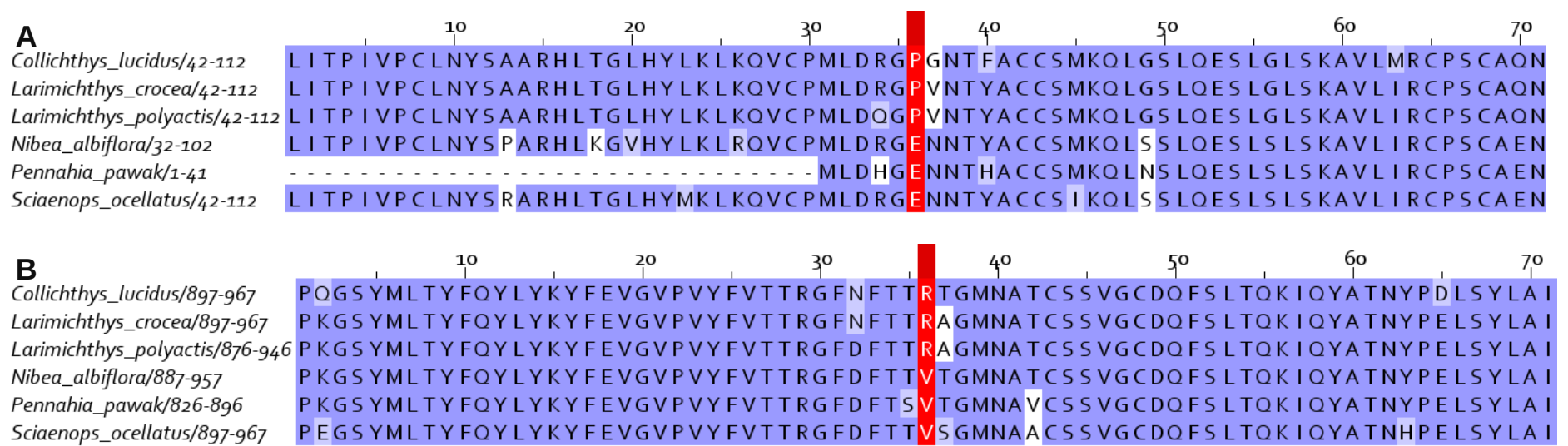
A
10 20 30 40 50 60 70
Collichthys_lucidus/42-112 LITPIVPCLNYSAARHLTGLHYLKLKQVCPMLDRGPGNTFACCSMKQLGSLQESLGLSKAVLMRCPSCAQN
Larimichthys_crocea/42-112 LITPIVPCLNYSAARHLTGLHYLKLKQVCPMLDRGPVNTYACCSMKQLGSLQESLGLSKAVLIRCPSCAQN
Larimichthys_polyactis/42-112 LITPIVPCLNYSAARHLTGLHYLKLKQVCPMLDQGPVNTYACCSMKQLGSLQESLGLSKAVLIRCPSCAQN
Nibea_albiflora/32-102 LITPIVPCLNYSPARHLKGVHYLKLRQVCPMLDRGENNTYACCSMKQLSSLQESLSLSKAVLIRCPSCAEN
Pennahia_pawak/1-41 ----------MLDHGENNTHACCSMKQLNSLQESLSLSKAVLIRCPSCAEN
Sciaenops_ocellatus/42-112 LITPIVPCLNYSRARHLTGLHYMKLKQVCPMLDRGENNTYACCSIKQLSSLQESLSLSKAVLIRCPSCAEN
B
10 20 30 40 50 60 70
Collichthys_lucidus/897-967 PQGSYMLTYFQYLYKYFEVGVPVYFVTTRGFNFTTRTGMNATCSSVGCDQFSLTQKIQYATNYPDLSYLAI
Larimichthys_crocea/897-967 PKGSYMLTYFQYLYKYFEVGVPVYFVTTRGFNFTTRAGMNATCSSVGCDQFSLTQKIQYATNYPELSYLAI
Larimichthys_polyactis/876-946 PKGSYMLTYFQYLYKYFEVGVPVYFVTTRGFDFTTRAGMNATCSSVGCDQFSLTQKIQYATNYPELSYLAI
Nibea_albiflora/887-957 PKGSYMLTYFQYLYKYFEVGVPVYFVTTRGFDFTTVTGMNATCSSVGCDQFSLTQKIQYATNYPELSYLAI
Pennahia_pawak/826-896 PKGSYMLTYFQYLYKYFEVGVPVYFVTTRGFDFTSVTGMNAVCSSVGCDQFSLTQKIQYATNYPELSYLAI
Sciaenops_ocellatus/897-967 PEGSYMLTYFQYLYKYFEVGVPVYFVTTRGFDFTTVSGMNAACSSVGCDQFSLTQKIQYATNHPELSYLAI

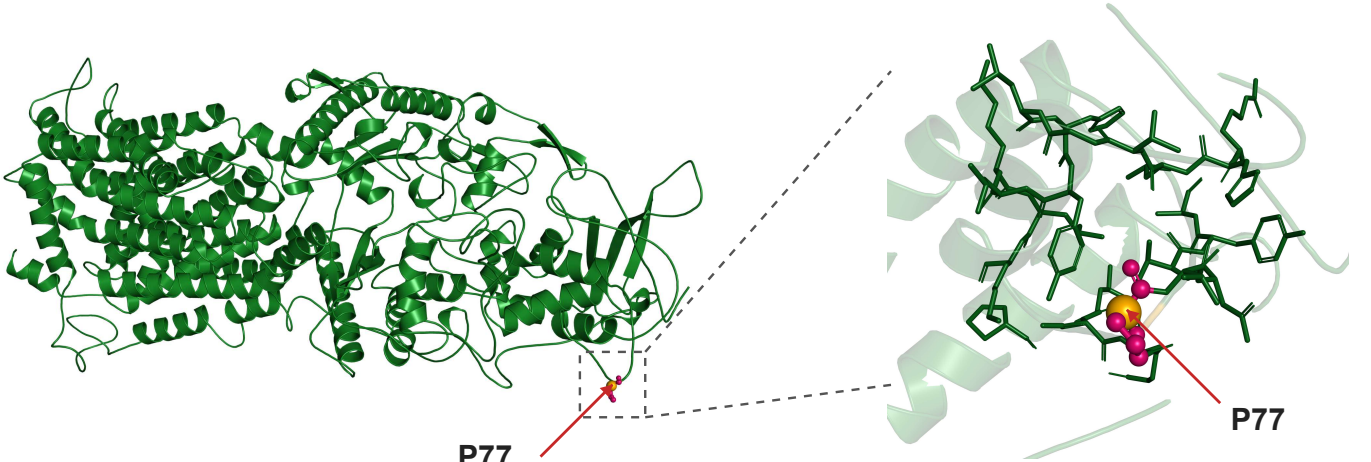
P77
P77

(A) Dietary carotenoid uptake in fish intestine

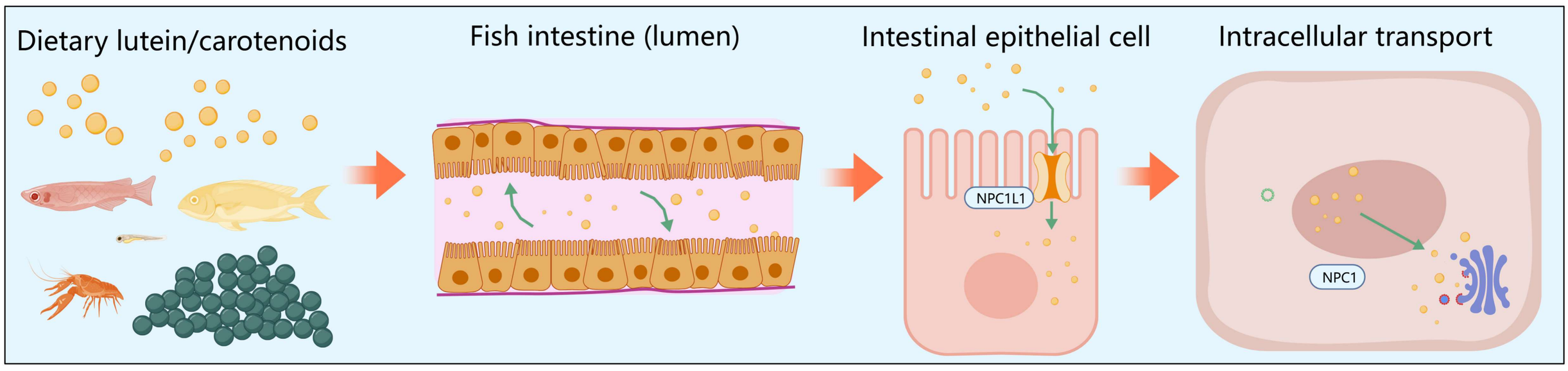

(B) Lipid-mediated carotenoid transport and redistribution

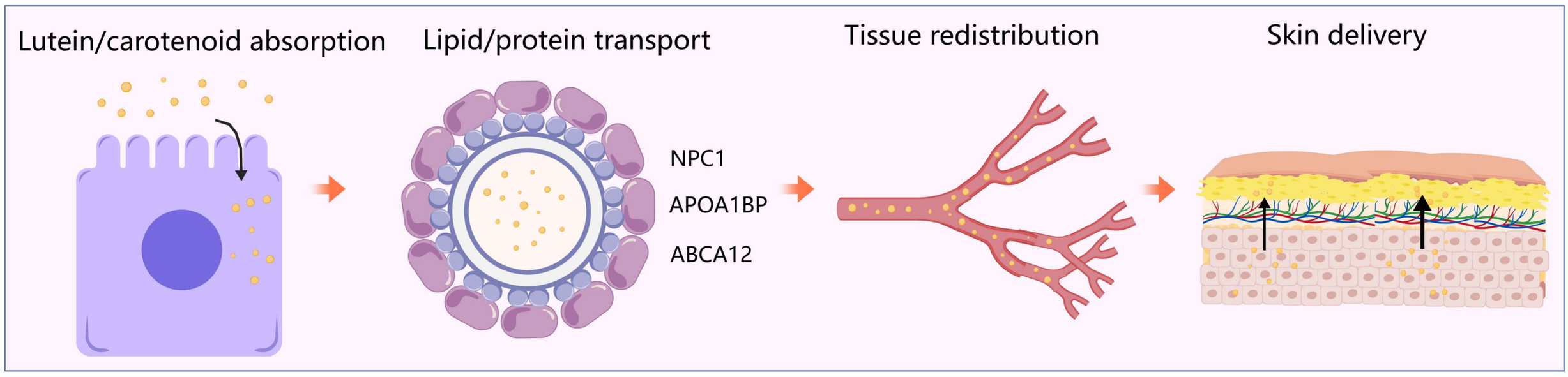

(C) Carotenoid storage in xanthophores and lipid droplets

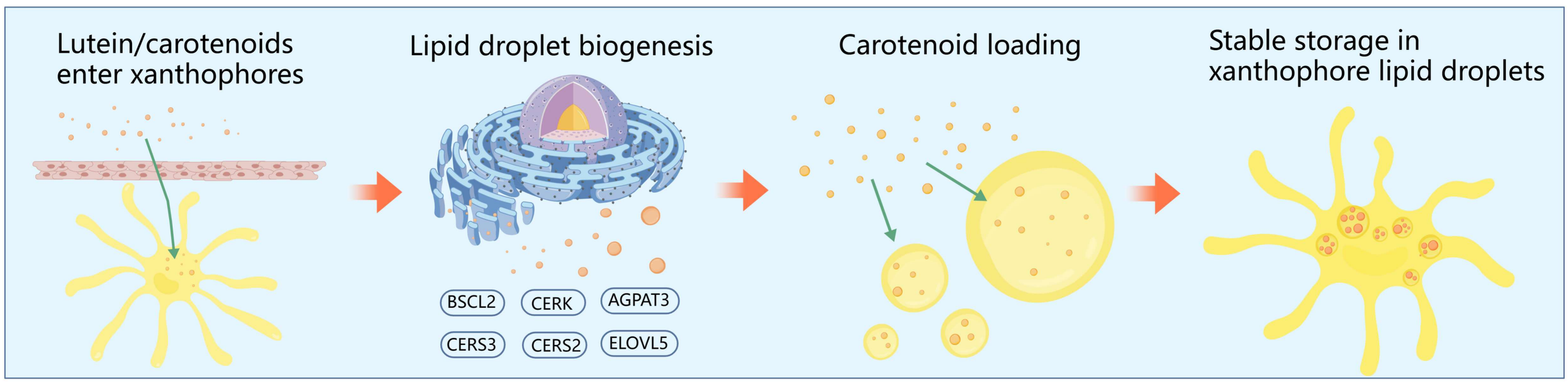

(D) Melanin masking reduction and optical enhancement

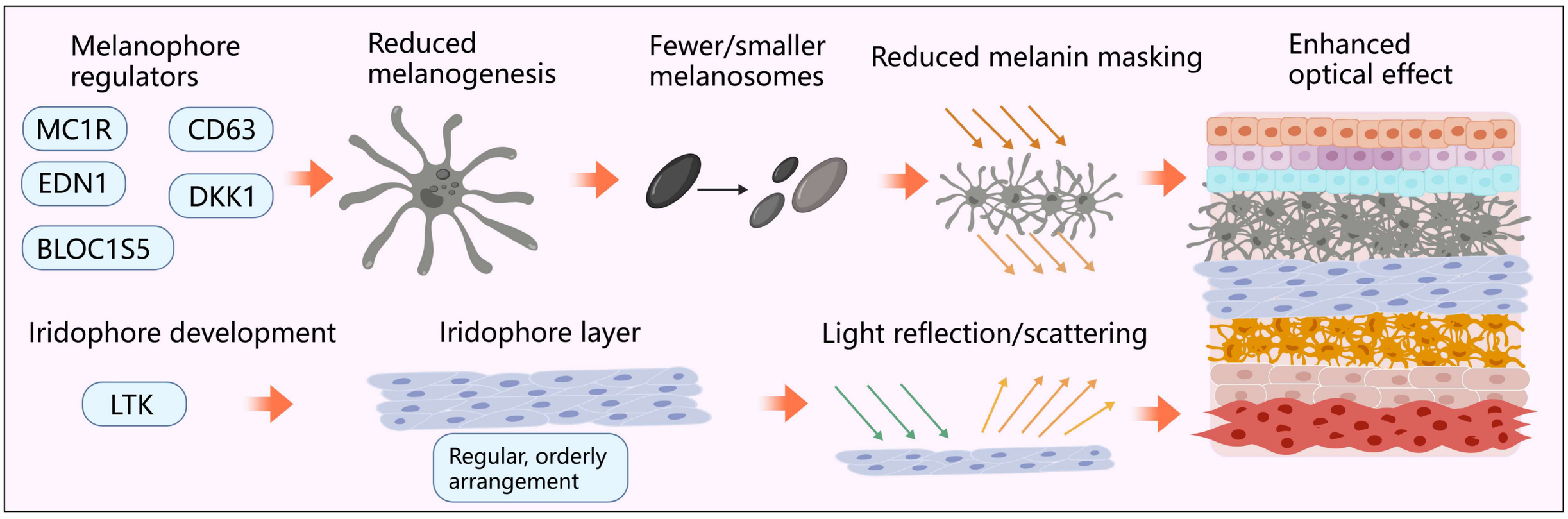
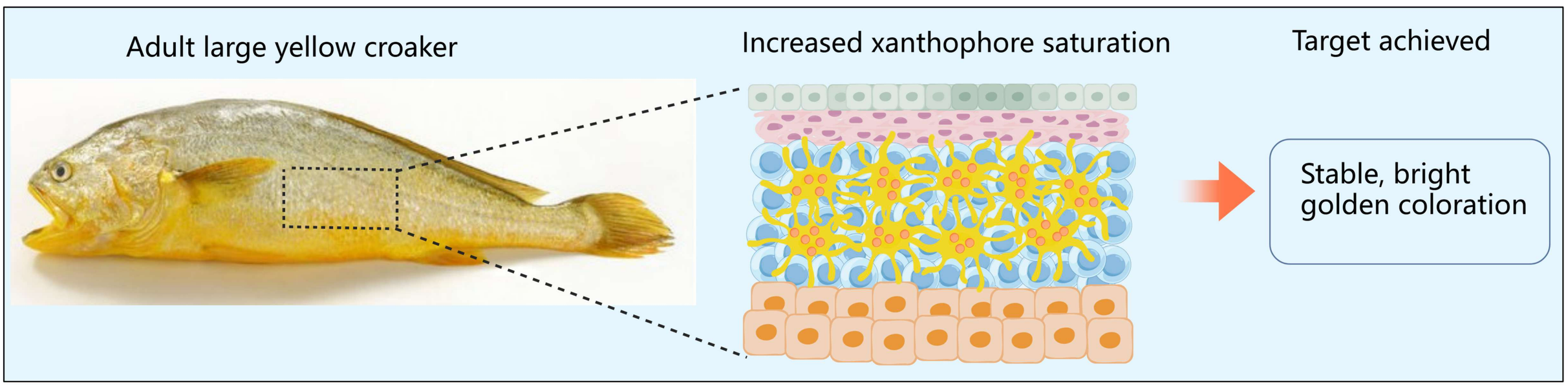
(E) Effect on adult large yellow croaker coloration